Crystallization of Homopolymers Confined in Spherical or Cylindrical Nanodomains

Shuichi Nojima,*,† Yuya Ohguma,† Shingo Namiki,† Takashi Ishizone,† and Kazuo Yamaguchi‡

Department of Organic and Polymeric Materials, Graduate School of Science and Engineering, Tokyo Institute of Technology, H-125, 2-12-1 Ookayama, Meguro-Ku, Tokyo 152-8552, Japan, and Department of Chemistry, Faculty of Science, Kanagawa University, Hiratsuka, Kanagawa 259-1293, Japan

Received December 14, 2007

Revised Manuscript Received January 29, 2008

Introduction. Spatially confined crystallization observed in crystalline block copolymers provides an interesting research subject from the viewpoint of nanostructural control in polymer materials.[1] It is well-known that isolated nanodomains (i.e., spheres or cylinders) affect the crystallization of constituent blocks to yield a considerable decrease in the crystallization temperature and crystallinity,[2−7] where we can consider two principal factors which simultaneously affect the crystallization process: (1) spatial confinement by nanodomains surrounding the crystalline blocks and (2) chain confinement by tethering at the nanodomain interface (Figure 1a). In order to understand the effects of these factors separately on the crystallization behavior, it is necessary to prepare such a system where *crystalline homopolymers* are confined within spherical or cylindrical nanodomains (Figure 1b) and to investigate the differences in crystallization behavior between two systems (a/b or b/c in Figure 1).

It is not easy to prepare such a system, and new ideas are necessary to do it. Ho et al.[8] studied the crystallization behavior of poly(ϵ-caprolactone) (PCL, $[-(CH_2)_5-CO-O-]_n$) homopolymers in a binary blend of PCL and polystyrene-*block*-poly(ethylene−propylene) (PS-*b*-PEP), where PCL was localized between microphase-separated PS-*b*-PEP layers and eventually confined within lamellar nanodomains consisting of PS and PEP layers. They concluded that the melting temperature, crystallinity, and crystallization rate of confined PCL were significantly different from those of bulk PCL without any spatial confinement. Recently some research groups studied the crystallization of homopolymers confined in nanoporous alumina and reported the interesting relationship between the crystallization behavior and the properties of nanorods.[9−11] Some computer simulations have also been performed for homopolymer crystallization in isolated nanodomains.[12,13]

In this Communication, we report the crystallization behavior of poly(δ-valerolactone) (PVL) homopolymers ($[-(CH_2)_4-CO-O-]_n$) spherically or cylindrically confined within PS matrices and emphasize differences in crystallization between PVL blocks (Figure 1a) and PVL homopolymers (Figure 1b). The systems were prepared by the microphase separation of PVL-*b*-PS copolymers followed by photocleavage at block junctions to yield PVL homopolymers confined within PS nanodomains.

* Corresponding author: Ph +81-3-5734-2132; Fax +81-3-5734-2888; e-mail snojima@polymer.titech.ac.jp.

† Tokyo Institute of Technology.

‡ Kanagawa University.

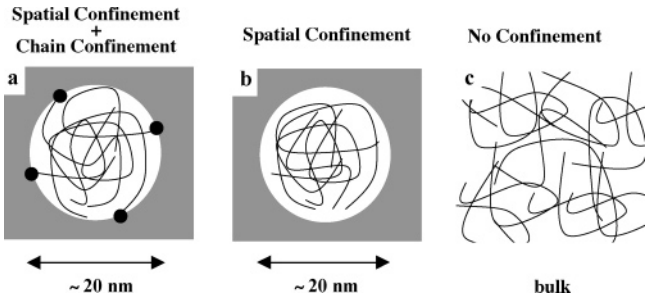

Figure 1. Schematic illustration showing crystalline blocks and crystalline homopolymers confined within a spherical nanodomain (a and b) and crystalline homopolymers without any spatial confinement (c).

Experimental Section. a. Samples. We prepared two PVL-*b*-PS copolymers with a photocleavable *o*-nitrobenzyl group[14] between PVL and PS blocks. The glass transition temperature of PS is ca. 100 °C, and the melting temperature of PVL is ca. 45 °C (Figure 3a), so that the vitrification of PS chains prevents macrophase separation between PS and PVL homopolymers after photocleavage at temperatures where PVL crystallizes, and eventually we can observe the crystallization of PVL homopolymers confined within the PS nanodomain originally formed by the microphase separation of PVL-*b*-PS copolymers. The methods of sample synthesis and characterization will soon appear. Table 1 shows the molecular characteristics of samples used in this study. The number after V (or S) in the sample code represents the molecular weight of PVL (or PS) chains in kg/mol, and "−" stands for samples before photocleavage, i.e., normal diblock copolymers, while "/" for those after photocleavage, i.e., PVL homopolymers confined within PS matrices.

The crystal structure of PVL was recently reported by Furuhashi et al.,[15] and it is very close to that of PCL. For example, the specific volume of PVL crystals is 0.840 cm^3/g and that of PCL crystals 0.833 cm^3/g.[16] However, the specific volume of amorphous PVL is not found in the literature, so we used the specific volume of amorphous PCL[17] to obtain the volume fraction of PVL in the system. For the specific volume of PS we used the value reported by Richardson and Savill.[18]

b. Photocleavage. UV with 1000 mW/cm^2 in intensity and wavelength longer than 300 nm was irradiated for 3 min to thin films with ca. 50 μm in thickness to cleave the block junction. This photocleaving process is completely irreversible; i.e., once the junction is broken it never recombines into copolymers, which is advantageous for our crystallization experiments.[19] The samples before and after UV irradiation were examined by gel permeation chromatography (GPC), and the photocleavage yield was evaluated from the ratio of peak areas of PVL-*b*-PS copolymers and PS homopolymers. The yield was 72% for V8/S21 and 88% for V6/S42, and therefore a small amount of PVL blocks remained in the system after photocleavage. This fact does not imply that the system has two nanodomains, one consisting of PVL homopolymers and the other PVL blocks, but the PVL blocks will be distributed uniformly in every nanodomain because the DSC curve showed a single endothermic peak during heating. Therefore, we can expect the effect of chain confinement on the crystallization behavior even for 72% or 88% photocleaved systems.

c. Small-Angle X-ray Scattering (SAXS). The microdomain structures before and after photocleavage at selected temperatures were investigated by SAXS using synchrotron radiation,

10.1021/ma7027903 CCC: $40.75
Published on Web 02/19/2008

Table 1. Characterization of Samples Used in This Study

sample code	$M_n \times 10^{-3}$ PVL	$M_n \times 10^{-3}$ PS	ϕ_{PVL} (wt %)	M_w/M_n	f_{pc}[a] (%)	morphology[b]
V8−S21	8.5	21	29	1.04	0	cylinder
V8/S21	8.5	21	29	1.04	72	cylinder
V6−S42	6.4	42	12	1.02	0	sphere
V6/S42	6.4	42	12	1.02	88	sphere

[a] Photocleavage yield obtained by GPC. [b] Determined by SAXS.

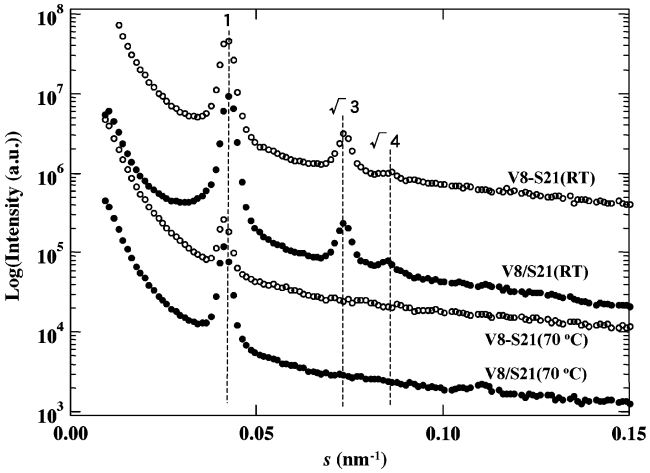

Figure 2. SAXS curves for V8−S21 (before photocleavage, open circles) and V8/S21 (after photocleavage, closed circles) at room temperature (top two curves) and 70 °C ($> T_m$, bottom two curves). The plots of the data for V8−S21(RT), V8/S21(RT), and V8−S21(70 °C) are shifted upward successively for legibility.

which was performed at Photon Factory in high energy accelerator research organization, Tsukuba Japan, with a small-angle X-ray equipment for solution (SAXES) installed at beamline BL-10C. Details of the equipment and the instrumentation are described in our previous publications.[20−23] The scattered intensity was recorded with a one-dimensional position-sensitive proportional counter (PSPC), by which isotropic scattering from the sample was obtained as a function of s (= $(2/\lambda)$ sin θ, λ is the X-ray wavelength (= 0.1488 nm) and 2θ the scattering angle). The spacing, an alternating period of the structure, was evaluated from the angular position of the primary intensity peak.

d. Differential Scanning Calorimetry (DSC). A Perkin-Elmer DSC Diamond was employed with a heating rate of 20 °C/min to obtain the melting temperature and crystallinity of PVL chains crystallized at selected temperatures for a long time. Actually the heat of fusion for PVL chains was used instead of crystallinity because that for perfect PVL crystals was not found in the literature. We also investigated the crystallization behavior of each sample by DSC. The samples crystallized at selected crystallization temperature T_c (-52 °C $\le T_c \le -48$ °C for V8−S21 and V8/S21 and -67 °C $\le T_c \le -61$ °C for V6−S42 and V6/S42) for prescribed times t_c were quickly transferred to a higher temperature (∼15 °C), where further crystallization of PVL did not occur, and then heated at 20 °C/min until PVL melted completely. The endothermic heat of melting was evaluated as a function of t_c to compare the crystallization behavior among each sample.

Results and Discussion. Figure 2 shows SAXS curves for V8−S21 and V8/S21 at room temperature (where PVL is crystallized) and those at 70 °C (PVL is amorphous). The SAXS curves at room temperature have a few scattering peaks, and the angular positions of these peaks exactly correspond to the ratio of 1:$\sqrt{3}$:$\sqrt{4}$, indicating that the PVL cylindrical microdomain is formed in PS matrices. On the basis of the composition, the specific volume of each block, and the primary peak position of SAXS curves, the diameter of this cylinder is estimated to be 15.7 nm. Similar consideration leads that V6−S42 and V6/S42 have a spherical microdomain structure with a 17.6 nm diameter. The SAXS curves at 70 °C, where PVL is amorphous, show a similar pattern with the primary peak position being unchanged though the higher order peaks are unclear because of small difference in electron density between amorphous PVL (= 344 e/nm^3 at 70 °C, estimated from the specific volume of amorphous PCL) and amorphous PS (= 338 e/nm^3 at 70 °C). This fact indicates clearly that the cylindrical or spherical microdomains are completely preserved in V8/S21 and V6/S42 even after the melting of PVL homopolymers. In addition, the samples remained transparent after photocleavage, suggesting no macroscopic phase separation between PVL and PS homopolymers due to the vitrification of PS matrices. Therefore, we can investigate differences in crystallization behavior between PVL blocks and PVL homopolymers on identical crystallization conditions.

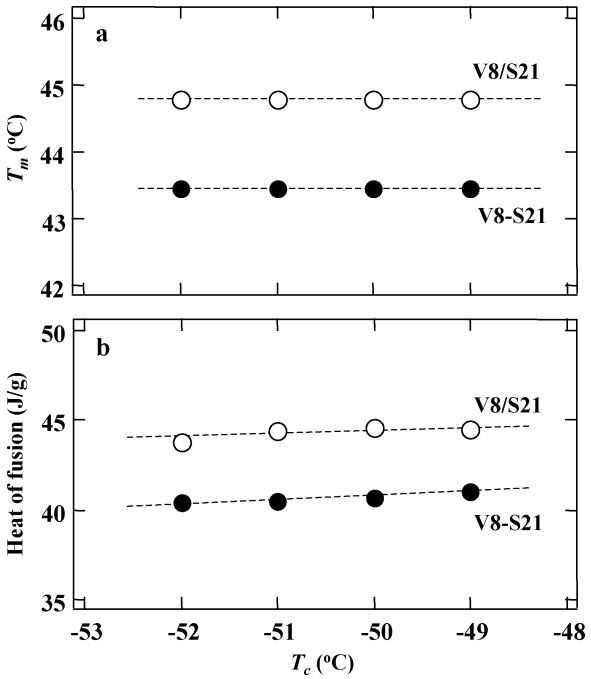

Figure 3. T_m (a) and ΔH per 1 g PVL (b) (proportional to crystallinity) plotted against T_c for PVL homopolymers in V8/S21 (open circles) and PVL blocks in V8−S21 (closed circles).

The melting temperature T_m and heat of fusion ΔH (proportional to crystallinity) of PVL chains are plotted against T_c in Figure 3 for V8−S21 and V8/S21. T_m and ΔH for V8/S21 are significantly higher than those for V8−S21, indicating that the PVL homopolymer has a higher crystallizability than the PVL block in the same nanodomain. This fact is recently predicted by Monte Carlo simulations for a cylindrically confined system,[12] where crystal orientations are perpendicular to the cylinder axis for tethered blocks while they are parallel for homopolymers resulting in large differences in the crystal thickness and crystallinity. Figure 3 also shows that T_m and ΔH are almost independent of T_c. In crystalline homopolymers both values usually increase steadily with increasing T_c.[24] The spatial restriction does not permit more favorable crystallization or relaxation on a long time scale, for example lamella thickening, with increasing T_c.

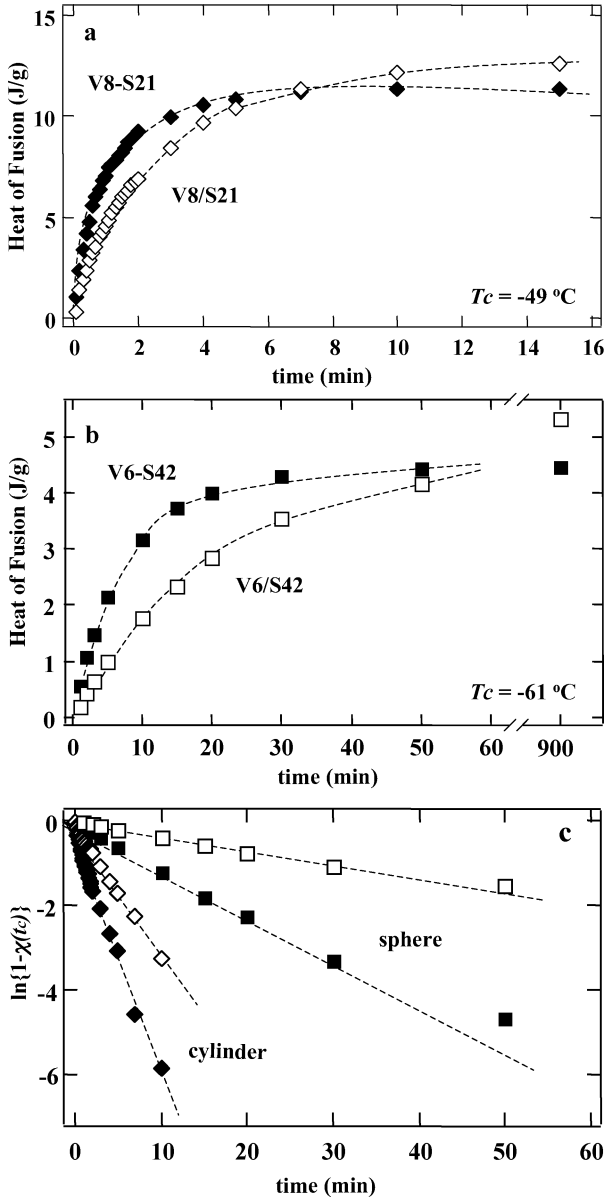

Figure 4. ΔH per 1 g sample plotted against t_c for PVL homopolymers (open symbols) and PVL blocks (closed symbols) confined in cylindrical nanodomains (a) and spherical nanodoamins (b). The crystallization temperature is shown in each panel. (c) $\ln\{1 - \chi(t_c)\}$ plotted against t_c for each crystallization process, where the symbols are the same as those in panels a and b.

We pursued isothermal crystallization of PVL blocks and PVL homopolymers by DSC as the time evolution of ΔH. Figures 4a,b are the plots of ΔH vs t_c and show differences in the crystallization behavior between PVL blocks and PVL homopolymers in cylindrical or spherical nanodomains on identical crystallization conditions, where the plots show a steep increase at early stage crystallization followed by an asymptotic increase at late stage. This time evolution is extremely different from that usually observed in crystalline homopolymers, where we can observe *sigmoid*-shaped time evolution. Figures 4a,b resemble the crystallization behavior (for example, time evolution of primary peak intensity in SAXS curves) of constituent blocks confined in self-assembled spherical nanodomains formed in rubbery crystalline diblocks,[3−5,25,26] where total crystallization shows the nucleation-controlled process or first-order process. That is, the crystallization rate at t_c is proportional to the volume fraction of uncrystallized domains remaining at t_c. Therefore, the plot of $\ln\{1 - \chi(t_c)\}$ vs t_c ($\chi(t_c)$: normalized crystallinity at t_c) should give a straight line, and the slope is a measure for the crystallization rate of this process.[27] Note that this plot exactly corresponds to $n = 1$ in Avrami equation. Figure 4c shows such plots for all samples investigated, where the crystallization rate (or the slope in Figure 4c) of cylindrically confined chains (homopolymers or blocks) are extremely larger than that of spherically confined polymers. In addition, the crystallization rate of PVL blocks is ca. 2.4 or 3.4 times larger than that of PVL homopolymers in cylindrical or spherical nanodomains, respectively. In summary, the total crystallization of cylindrically or spherically confined PVL homopolymers as well as PVL blocks can be described by the first-order process, and we can observe the significant differences in crystallization rate between them.

We pursued the nucleation rate in Figures 4a,b since the growth rate should be extremely fast owing to small domains. Therefore, these figures indicate clearly that the crystallization occurs predominantly at the nanodomain interface because the only difference in crystallization between PVL blocks and PVL homopolymers is whether one end of PVL chains is tethered at the domain interface or not. This difference yields the difference in the thermal motion of the chain end; tethered chains have slower thermal motion than free chains, leading to a larger possibility to form a nucleus. This kind of interfacial nucleation is reported in various systems such as homopolymers confined in micrometer domains,[27] immiscible polymer blends,[28] and spherically or cylindrically confined block copolymers.[3−5,25,26] Predominant nucleation at microdomain interfaces is also confirmed by molecular dynamics simulations. Miura and Mikami,[13] for example, showed that the domain interface accelerated the crystallization rate of semiflexible homopolymers confined in isolated nanodomains because of the activated nucleation process at domain interfaces. These simulation results as well as other experimental results strongly support our conclusion; i.e., nucleation occurs predominantly at the domain interface.

In this Communication, we mainly described differences in crystallization between PVL homopolymers and PVL blocks confined in isolated nanodomains (Figures 1a,b). Differences in crystallization between spatially confined homopolymers and bulk homopolymers (Figures 1b,c), on the other hand, will provide fundamental effects of isolated nanodomains on the crystallization of flexible homopolymers. The difference in crystallization behavior between these systems is, however, extremely large compared to that between confined blocks and homopolymers. For example, the crystallization temperature of confined homopolymers (and also blocks) is considerably lower than that of bulk homopolymers (ca. 80° difference), and the crystallinity is significantly small.[5] These facts indicate that the isolated nanodomains (sphere or cylinder) strongly restrict the crystallization of polymer chains inside. The effect of chain tethering at domain interfaces is smaller, but it is not negligible when we consider the crystallization behavior of flexible chains confined within isolated nanodomains.

Acknowledgment. This work was supported in part by NEDO (New Energy and Industrial Technology Development Organization) launched in 2001 and also by Grants-in-Aid for Scientific Research on Basic Areas (B) (No. 17350102) from the Ministry of Education, Science, Sports, and Culture of Japan. The SAXS measurement has been performed under the approval of Photon Factory Advisory Committee (No. 2006G078).

References and Notes

(1) Muller, A. J.; Balsamo, V.; Arnal, M. L. *Adv. Polym. Sci.* **2005**, *190*, 1.

(2) Weimann, P. A.; Hajduk, D. A.; Chu, C.; Chaffin, K. A.; Brodil, J. C.; Bates, F. S. *J. Polym. Sci., Part B* **1999**, *37*, 2053.
(3) Loo, Y. L.; Register, R. A.; Ryan, A. J. *Phys. Rev. Lett.* **2000**, *84*, 4120.
(4) Loo, Y. L.; Register, R. A.; Ryan, A. J.; Dee, G. T. *Macromolecules* **2001**, *34*, 8968.
(5) Nojima, S.; Toei, M.; Hara, S.; Tanimoto, S.; Sasaki, S. *Polymer* **2002**, *43*, 4087.
(6) Balsamo, V.; Navarro, C. U.; Gil, G. *Macromolecules* **2003**, *36*, 4507.
(7) Lorenzo, A. T.; Arnal, M. L.; Muller, A. J.; Fierro, A. B.; Abetz, V. *Eur. Polym. J.* **2006**, *42*, 516.
(8) Ho, R. M.; Chiang, Y. W.; Lin, C. C.; Huang, B. H. *Macromolecules* **2005**, *38*, 4769.
(9) Steinhart, M.; Goring, P.; Dernaika, H.; Prabhukaran, M.; Gosele, U.; Hempel, E.; Thurn-Albrecht, T. *Phys. Rev. Lett.* **2006**, *97*, 027801.
(10) Woo, E.; Huh, J.; Jeong, Y. G.; Shin, K. *Phys. Rev. Lett.* **2007**, *98*, 136103.
(11) Wu, H.; Wang, W.; Yang, H.; Su, Z. *Macromolecules* **2007**, *40*, 4244.
(12) Wang, M.; Hu, W.; Ma, Y.; Ma, Y. Q. *J. Chem. Phys.* **2006**, *124*, 244901.
(13) Miura, T.; Mikami, M. *Phys. Rev. E* **2007**, *75*, 031804.
(14) Yamaguchi, K.; Kitabatake, T.; Izawa, M.; Fujiwara, T.; Nishimura, H.; Futami, T. *Chem. Lett.* **2000**, *29*, 228.
(15) Furuhashi, Y.; Sikorski, P.; Atkins, E.; Iwata, T.; Doi, Y. *J. Polym. Sci.*, Part B **2001**, *39*, 2622.
(16) Chatani, Y.; Okita, Y.; Tadokoro, H.; Yamashita, Y. *Polym. J.* **1970**, *1*, 555.
(17) Crescenzi, V.; Manzini, G.; Calzolari, G.; Borri, C. *Eur. Polym. J.* **1972**, *8*, 449.
(18) Richardson, M. J.; Savill, N. G. *Polymer* **1977**, *18*, 3.
(19) Goldbach, J. T.; Lavery, K. A.; Penelle, J.; Russell, T. P. *Macromolecules* **2004**, *37*, 9639.
(20) Nojima, S.; Kato, K.; Ono, M.; Ashida, T. *Macromolecules* **1992**, *25*, 1922.
(21) Nojima, S.; Kato, K.; Yamamoto, S.; Ashida, T. *Macromolecules* **1992**, *25*, 2237.
(22) Nojima, S.; Kikuchi, N.; Rohadi, A.; Tanimoto, S.; Sasaki, S. *Macromolecules* **1999**, *32*, 3727.
(23) Nojima, S.; Kiji, T.; Ohguma, Y. *Macromolecules* **2007**, *40*, 7566.
(24) Wunderlich, B. *Macromolecular Physics. 2: Crystal Nucleation, Growth, Annealing*; Academic Press: New York, 1976.
(25) Chen, H. L.; Wu, J. C.; Lin, T. L.; Lin, J. S. *Macromolecules* **2001**, *34*, 6936.
(26) Zhu, L.; Mimnaugh, B. R.; Ge, Q.; Quirk, R. P.; Cheng, S. Z. D.; Thomas, E. L.; Lotz, B.; Hsiao, B. S.; Yeh, F.; Liu, L. *Polymer* **2001**, *42*, 9121.
(27) Massa, M. V.; Dalnoki-Veress, K. *Phys. Rev. Lett.* **2004**, *92*, 255509.
(28) Arnal, M. L.; Matos, M. E.; Morales, R. A.; Santana, O. O.; Muller, A. J. *Macromol. Chem. Phys.* **1998**, *199*, 2275.

MA7027903